

# An overheight vehicle–bridge collision monitoring system using piezoelectric transducers

G Song<sup>1</sup>, C Olmi and H Gu

Smart Materials and Structures Laboratory, Department of Mechanical Engineering,  
University of Houston, Houston, TX 77204, USA

E-mail: [gsong@uh.edu](mailto:gsong@uh.edu)

Received 12 July 2006, in final form 4 January 2007

Published 14 February 2007

Online at [stacks.iop.org/SMS/16/462](http://stacks.iop.org/SMS/16/462)

## Abstract

With increasing traffic volume follows an increase in the number of overheight truck collisions with highway bridges. The detection of collision impact and evaluation of the impact level is a critical issue in the maintenance of a concrete bridge. In this paper, an overheight collision detection and evaluation system is developed for concrete bridge girders using piezoelectric transducers. An electric circuit is designed to detect the impact and to activate a digital camera to take photos of the offending truck. Impact tests and a health monitoring test were conducted on a model concrete bridge girder by using three piezoelectric transducers embedded before casting. From the experimental data of the impact test, it can be seen that there is a linear relation between the output of sensor energy and the impact energy. The health monitoring results show that the proposed damage index indicates the level of damage inside the model concrete bridge girder. The proposed overheight truck–bridge collision detection and evaluation system has the potential to be applied to the safety monitoring of highway bridges.

(Some figures in this article are in colour only in the electronic version)

## 1. Introduction

One of the common structural problems in existing highway bridges is the damage at the bottom corners or edges of the reinforced concrete beams or box girders induced by an impact of trucks exceeding the allowable height clearance of the bridges. There is a pressing need to have an overheight collision protection system to identify the occurrence and level of such impact damage and thus ensure the integrity of bridge structures. Intelligent, or smart, materials are providing new solutions to old problems, such as overheight truck–bridge collision, with their advantages over current technology. Piezoelectric materials, one class of smart materials, have the advantages of being lightweight, relatively inexpensive and easy to implement. Building upon existing research in piezoelectric materials as force sensors, a new impact force detection system for the health monitoring of large-scale concrete structures, such as highway bridges, can be

developed to incorporate the advantages of the new materials and to provide better solutions to the overheight truck–bridge collision problem.

In recent years, some scholars have conducted research regarding impact testing with piezoelectric transducers. Lorenz *et al* (1994) have designed and calibrated an impact penetrometer using a piezoelectric transducer for use on a spacecraft scheduled to land on the surface of Titan, one of Saturn's moons. The impact force profile allows estimation of the density and cohesion of the surface material and its particle size distribution. Lee *et al* (1998) designed and built an ultra-high-precision high-speed piezoelectric impact system. The experimental data indicates that this piezoelectric impact hammer has a timing accuracy in the range of microseconds and a positioning accuracy in the range of micrometres. The short impact time achieved by the impact hammer also warrants a high-frequency excitation achievable by the impact hammer. Tong *et al* (2002) designed and fabricated a piezoelectric impact hammer for nondestructive evaluation

<sup>1</sup> Author to whom any correspondence should be addressed.

of concrete structures. Due to the stable impact generation of the piezoelectric impact hammer, the experimental results showed that the accuracy of the wave velocity measurement was enhanced significantly through signal averaging. The accurate impact time origin has been determined by embedding a tiny piezoelectric sensor in the flying head. Measurements of the longitudinal and Rayleigh wave velocities of a concrete specimen were conducted. The newly designed impact hammer can be utilized to measure the depth of a normal surface-breaking crack in a concrete specimen.

Piezoelectric materials have also been successfully applied to the health monitoring of concrete structures. Many of the conventional nondestructive evaluation (NDE) methods such as C-scan, x-ray, etc., require accessibility to the inspected structural components and usually involve bulky equipment. The piezoelectric material-based health monitoring method has provided a promising approach for health monitoring of large-scale concrete structures. Ayres *et al* (1998) utilized the electrical impedance of a bonded piezoelectric actuator/sensor as a means to qualitatively detect structural damage and actively monitor a structure's integrity. This technique is highly sensitive to local damage in the sensing area. Tseng and Wang (2004) presented a smart, piezoelectric transducer-based method that is being developed to detect the presence of damage and monitor its progression in concrete structures. The frequency-dependent electric admittance signatures of the piezoelectric transducer are compared with the baseline signatures to determine the health status of the structures. The damage is quantified by the root-mean-square deviation (RMSD) index. Saafi and Sayyah (2001) attached an array of piezoelectric transducers to a structure to detect and localize disbands and delamination of advanced composite reinforcement from concrete structures. The authors compared the transfer function of the damaged structure with the undamaged structure to detect the disbond and delamination. Wang *et al* (2001) studied the Lamb wave-based health monitoring of both fibre-reinforced composites and steel-reinforced concrete. For health monitoring of steel-reinforced concrete, a piezoelectric sensor network was installed in selected rebars in areas such as the deck, the columns of bridges and the footing area of columns. Experimental results showed that the cracks or debonding damage in reinforced concrete structures can be detected by the proposed built-in active sensing system. Piezoelectric materials can also be applied to health monitoring in other forms such as powder (Egusa and Iwasawa 1998) or film (Galea *et al* 1993). Wavelet transform is a useful signal-processing tool for health monitoring. Quek *et al* (2001) used the experimental dynamic response data obtained from piezoelectric sensors to locate the crack position in the beam. By estimating the wave arrival times based on theoretical flexural wave velocity, the approximate wavelet scale to process the data can be determined.

In this paper, an overheight truck–bridge impact detection and evaluation method based on piezoelectric material is presented. The proposed method can be divided into two sections: (a) overheight truck–bridge impact detection and image capturing system and (b) an impact evaluation and health monitoring system. This research takes advantage of early work by the authors (Song *et al* 2004, 2005).

In the previous work, the piezoelectric transducers were embedded into concrete to perform health monitoring by using wavelet packet analysis. In this research, not only were two piezoelectric transducers used for health monitoring purposes, but one additional piezoelectric transducer was used to detect impact force and an impact detection circuit was designed for activating a digital camera to take photos of the offending truck which initiated the accident. Data acquired by the piezoelectric impact transducer was analysed and the relation between the impact energy and the energy of the sensor signal was established from the experimental data. The proposed method has the potential to be applied to the *in situ* health monitoring and maintenance of bridge structures.

## 2. Background of piezoelectric transducers

The piezoelectric effect was discovered by Jacques and Pierre Curie in 1880. Piezoelectricity is a phenomenon exhibited by non-centrosymmetric crystals whereby an electric polarization (i.e. charge) is induced in the material upon the application of a stress. Conversely, it is the development of an induced strain which is directly proportional to an applied electric field. In piezoelectric materials, the elastic and electrical properties are coupled; mechanical and electrical parameters must therefore be involved in constituent relations. For a piezoelectric medium, the interaction between electrical and mechanical variables can be described by linear relations of the form

$$D = dT + \varepsilon^T E \quad (1a)$$

$$S = s^E T + dE, \quad (1b)$$

where  $D$  represents the electric displacement,  $S$  represents the strain,  $d$  represents the piezoelectric coefficient,  $\varepsilon^T$  is the dielectric constant,  $T$  is the stress,  $E$  is the electric field and  $s^E$  is the compliance. Equation (1a) describes the direct piezoelectric effect, where the piezoelectric material will generate an electric charge when subjected to mechanical stress, while equation (1b) describes the converse piezoelectric effect. The piezoelectric material could function as a sensor due to the direct piezoelectric effect and as an actuator due to the converse piezoelectric effect when subjected to an electric field.

At present, the most versatile and popular piezoelectric ceramic material is lead zirconate titanate (PZT). The popularity of lead zirconate titanate is due to its strong piezoelectric effect and high Curie point, as well as the wide range of properties it offers simply by making small changes in composition. PZT can be fabricated into different shapes to meet specific geometric requirements. PZT patches can often be used as both sensors and actuators which can then be integrated into structures. In the proposed impact detection and evaluation system, PZT patches are used as transducers embedded into the concrete before casting.

The open-circuit voltage  $v$  yielded by the PZT transducer when compressed with force  $F$  is

$$v = \frac{g_{33} F t}{A} \quad (2)$$

where  $A$  is the area of transducer,  $t$  is the thickness of the PZT transducer and  $g_{33}$  is the piezoelectric voltage constant. The

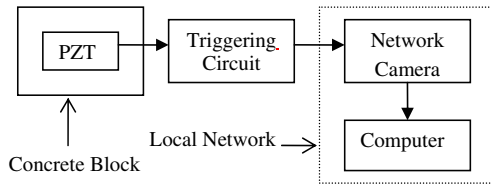


**Figure 1.** Block diagram of the impact detection and image capturing system.

piezoelectric voltage constant is defined as the electric field generated in a material per unit mechanical stress applied to it. The first subscript refers to the direction of the electric field generated in the material or to the applied electric displacement; the second refers, respectively, to the direction of the applied stress or to the direction of the induced strain. For all the tests conducted in this paper, the same type of PZT transducer in patch form is used. The area of the PZT transducer is 64 mm<sup>2</sup>, the thickness of the transducer is 0.267 mm and the piezoelectric voltage constant,  $g_{33}$ , is  $24 \times 10^{-3} \text{ V m N}^{-1}$ .

### 3. Overheight truck–bridge collision detection and image capturing system

#### 3.1. Experiment set-up

A concrete specimen was fabricated and used to simulate a bridge girder. This concrete specimen was embedded with PZT transducers. To detect the actual impact, a circuit was designed to read the PZT signal and output a trigger signal or an activating signal to an image capturing system at the moment of impact. To reduce the total cost of ownership (TCO), a commercial network camera, DCS3220 from D-Link, was used to take pictures of the offending vehicle. The camera is capable of capturing still images and sending them by e-mail or file transfer protocol (FTP) to a remote location. Also, an

integrated trigger input in the back of the camera allows the sending pictures to be based on the level of the input itself, providing a first-level filter of relevant images. To receive the images, a local networked computer with Serv-U FTP server software loaded was used. All networked components were connected using a Linksys router BEFSR41. Figure 1 shows the block diagram of the complete system.

For the actual simulation of impact, a modified radio controlled (RC) scaled tractor–trailer truck model was used to collide with the concrete specimen. The truck model was modified to create a stronger impact on the concrete block while not damaging itself in the process. The concrete block was elevated to about 6 inches from the ground to allow the truck to impact the lower area of the bridge. In addition to the RC truck, a modally impact hammer from PCB Piezoelectric Inc. model 086C03 was used to calibrate the force applied to the concrete block during the impact testing.

Labview 7.1 software with an NIDAQ 6251 PCI acquisition board and an SC2345 signal conditioning unit was used to capture relevant data from the circuit and the impact hammer. A total of three probes were used to capture the piezoelectric, the output trigger and the hammer signal.

#### 3.2. System and circuit design

Piezoelectric sensors output a voltage that is proportional to the mechanical stress applied to them. An electric circuit is to be designed and built to identify the maximum voltage level of the piezoelectric signal and compare it to a preset value. When the PZT signal does not exceed the preset value, the circuit will remain in a normal, low voltage state. If the impact signal is higher than the preset value, the circuit will change its output from low to high voltage and outputs a trigger or activating signal. Figure 2 shows the triggering circuit block diagram used in this experiment.

The internal capacitance of PZT sensors combined with an external resistive load, such as the one found in cables or bench instruments, is equivalent to a high pass filter.

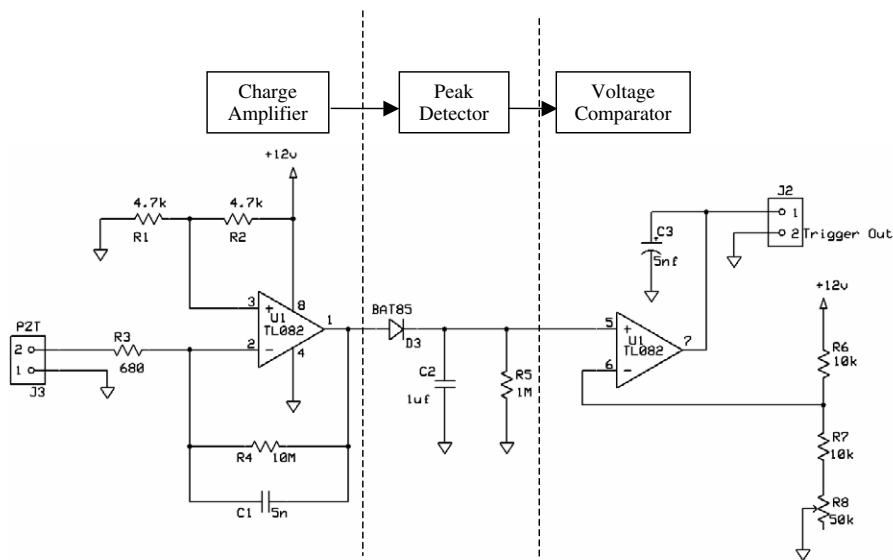


**Figure 2.** Triggering circuit block diagram and schematic.

To avoid reducing the signal strength at low frequencies, a charge amplifier design was used. The amplifier produces a voltage proportional to the input charge; thus, small changes in the input capacitance will not affect the output amplitude. The following equation describes the transfer function of the amplifier:

$$H(s) = -\frac{\tau_l s}{(\tau_h \tau_l) s^2 + (C_{PZT} R_3 + C_1 R_4) s + 1}, \quad (3)$$

where  $\tau_h$  and  $\tau_l$ , respectively, represent the higher and lower time constants that define the bandwidth of the amplifier. In the first case,  $\tau_h = R_3 C_1 = 3.4 \mu\text{s}$  or  $\frac{1}{\tau_h} \approx 294 \text{ kHz}$ , and in the second case  $\tau_l = R_4 C_{PZT} = 50 \text{ ms}$ , or  $\frac{1}{\tau_l} = 20 \text{ Hz}$ .

After amplifying the piezoelectric signal, the circuit identifies the highest voltage reached using a peak detector composed of a simple diode–capacitor combination. The last block in the triggering circuit compares the peak detector voltage to a preset voltage reference. The output will be at a high voltage when an impact is detected, and it will stay high for (Sendra and Smith 1998)

$$t = -R_5 C_2 \ln\left(\frac{V_{\text{ref}}}{V_{\text{pk}}}\right), \quad (4)$$

where  $V_{\text{ref}}$  is the preset voltage reference,  $V_{\text{pk}}$  and the product  $R_5 C_2$  are, respectively, the voltage detected and the time constant of the peak detector. The preset voltage reference should be used to change the impact sensibility of the circuit.

To actually capture the picture of the offending vehicle, the output of the triggering circuit was directly connected to the network camera trigger input. Through the web-based interface, the camera was set up to connect to the local computer and save a picture of the impact when a rise in voltage is detected at the trigger input. To accomplish the transfer of images, a local network was set up using a router and a FTP server on the local computer. To simplify the experiment set-up, administrator privileges were granted to the FTP client that will eventually connect to save the pictures.

### 3.3. Experiment results

After setting up the experiment, the radio controlled truck was collided several times with the concrete block. The signal generated by the piezoelectric sensor and the output trigger was recorded using Labview. During the pre-testing time, the RC truck did not create a strong enough impact. To detect the impact, the sensitivity of the circuit, or preset value, was adjusted. Through the following experiments, the preset voltage reference was experimentally found to be around 6 V for the specific PZT sensor and background noise of the lab. The specific value allowed the circuit to reject noise and random vibrations detected by the sensor. Preset values may change depending on the type of sensor, size of concrete block and minimum desired impact to be detected.

In the first impact after the pre-testing period, the circuit captured and processed the signal correctly. At the same time, the network camera took a picture of the ongoing impact. Figure 3 shows the signal detected by the PZT sensor and the output trigger signal from the circuit.

During the impact, the RC truck did not hit the concrete block perpendicularly, but with a small angle. Figure 3 shows

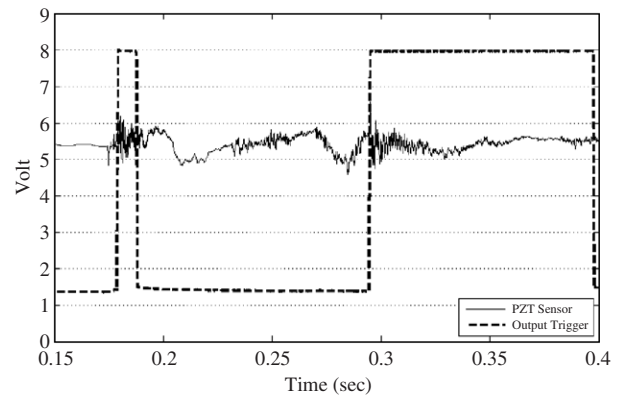


Figure 3. PZT sensor signal and output signal from the triggering circuit during an impact.



Figure 4. The acquired picture of overweight truck–bridge collision.

that the first impact happened approximately 120 ms before the final one. The length of the first impulse was not recognized by the network camera input. Unfortunately, the minimum trigger signal period value was not available from the manufacturer, but can be estimated at approximately 50 ms. The captured picture of the RC truck colliding with the model bridge girder is shown in figure 4.

In a second attempt, the RC truck was exchanged for an impact hammer, which outputs a signal proportional to the force applied to the concrete block. Figure 5 shows the hammer, the piezoelectric sensor and the trigger output signals. The maximum force applied by the hammer in this second attempt was 1501 N while the trigger signal was high for 64 ms. The force calculation was provided by the hammer resolution of  $2.25 \text{ mV N}^{-1}$ .

## 4. Impact evaluation and health monitoring system

### 4.1. Experimental set-up

A concrete beam  $101.6 \text{ mm} \times 914.4 \text{ mm} \times 19 \text{ mm}$  ( $4'' \times 36'' \times 0.75''$ ) was fabricated as a test object. Three piezoceramic patches (PZT1, PZT2 and PZT3) coated with waterproof coating were embedded into the concrete specimen before casting. The size of the piezoceramic patch is  $8 \text{ mm} \times 8 \text{ mm}$ . One piezoceramic transducer (PZT2) was used as the impact force detector to estimate the magnitude of the impact

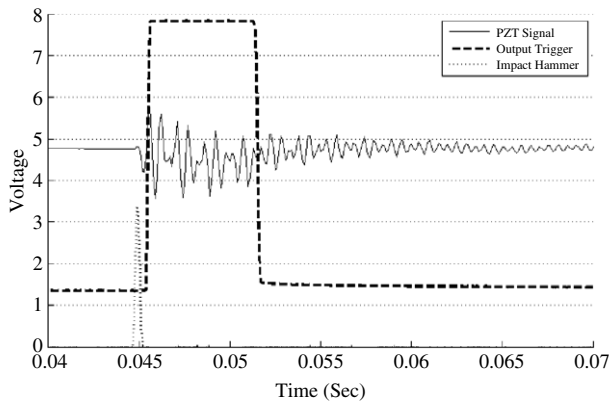


**Figure 5.** Impact hammer signal, PZT sensor output and output signal from the triggering circuit.

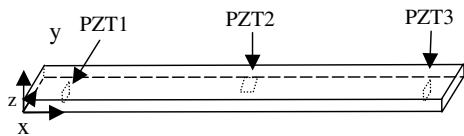


**Figure 6.** Concrete specimen instrumented with piezoceramic patches.

force and to trigger the photographing of the offending truck. Additionally, all three piezoceramic transducers were also used for health monitoring purposes. The level of damage was determined from the sensor signal by using the wavelet packet analysis. A damage index was defined on the basis of the energy vector of the decomposed signal on different frequency bands. A 4.7625 mm (0.1875”) diameter rebar was placed at the bottom of the concrete specimen. Figure 6 is a diagram of the concrete specimen instrumented with PZT transducers. The coordinates of the piezoceramic patches and the properties of the piezoceramic transducers are presented in tables 1 and 2.

The impact tests were comprised of two parts: (1) the impact hammer test and (2) the free dropping test. During the impact hammer test, an impact hammer was used to generate impulse impact at different peak values on the concrete specimen. The relationship between the sensor signal and the impulse signal is then analysed. In the free dropping test, two balls of different masses were dropped from different heights. The relationships between the output of impact sensor energy and the impact velocity and between the impact force were analysed. The experimental data showed that the outputted sensor energy is related to both the impact force and the impact velocity.

**4.2. Impact hammer test**

A modally tuned impact hammer (model no. 086C03, PCB Inc.), weighing 0.16 kg and with a sensitivity of 2.24 mV N<sup>-1</sup>, was used for the impact test. A LeCroy Waverunner digital oscilloscope (model No. LT 342) was used to record the impact signal and the sensor signal at the sampling frequency of 1 MHz. When the hammer impacts the concrete specimen, the impact impulse signal can be captured from one of the PZT transducers embedded inside the hammer. The output of the

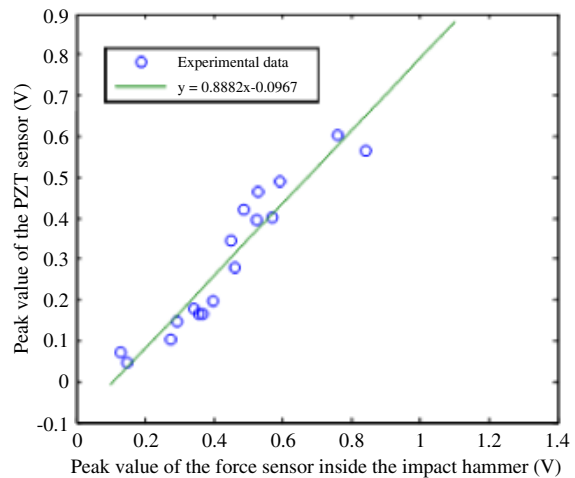


**Figure 7.** Peak voltage of the PZT sensor versus peak value of the force sensor inside the hammer.

**Table 1.** The coordinates and capacitance of the piezoceramic transducers (1 inch = 25.4 mm).

	X (inch)	Y (inch)	Z (inch)	Capacitance (nF)
PZT1	2	2	0.375	4.41
PZT2	18	2	0.375	4.21
PZT3	34	2	0.375	4.43

**Table 2.** Properties of the piezoceramic transducer.

Property coefficient		Unit	Value
Strain/field coefficient	$d_{33}$	m V <sup>-1</sup>	$390 \times 10^{-12}$
Strain/field coefficient	$d_{31}$	m V <sup>-1</sup>	$-190 \times 10^{-12}$
Strain/charge density coefficient	$g_{33}$	V N <sup>-1</sup> m <sup>-1</sup>	$24 \times 10^{-3}$
Strain/charge density coefficient	$g_{31}$	V N <sup>-1</sup> m <sup>-1</sup>	$-11.6 \times 10^{-3}$
Coupling coefficient	$k_{33}$		0.72
Coupling coefficient	$k_{31}$		0.35

hammer signal is proportional to the impact force. From the impact hammer experiment results (figure 7), it can be seen that the peak value of impact sensor is proportional to the peak value of the impact hammer. The peak value of the impact sensor can therefore be used to estimate the impact force peak value.

**4.3. Free dropping impact test**

To study the relationship between the impact energy and the sensor signal, free dropping impact tests were performed on the concrete specimen. The impact of a free dropping ball is considered as a point load for the concrete specimen. Two balls of differing mass were used for tests. The mass of one ball was 28 g, while the mass of the other ball was 242 g. Both balls were freely dropped from various heights at zero initial velocity. From the conservation of energy principle, the value of the kinetic energy upon impact should be equal to the potential energy loss from the dropping point. By adjusting the height, the impact kinetic energy is changed. The energy of the

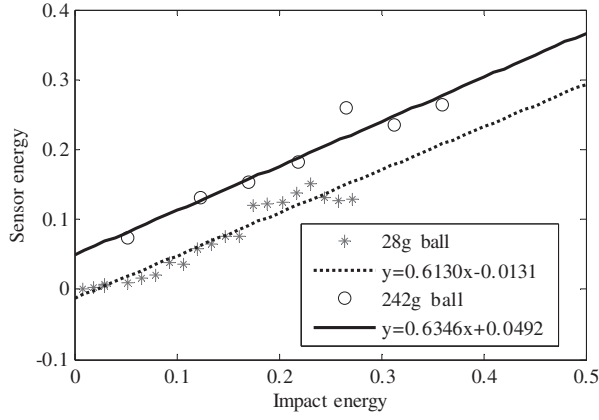


**Figure 8.** Sensor energy versus impact energy.

PZT impact sensor is calculated as

$$E = \int_{t_0}^{t_f} u^2 dt, \quad (5)$$

where  $t_0$  is the starting time,  $t_f$  is the finish time and  $u$  is the sensor voltage.

From figure 8, it can be seen that the relationship between the sensor energy and the impact energy is linearly proportional and the two curves have similar slope for different masses. For the same mass, higher impact energy correlated to higher impact velocity. With the increment of impact velocity, the impact energy increased, resulting in the proportional increment in the energy output of the impact sensor. The slope of the curve is related to the ratio of converting the mechanical energy to electrical energy by the PZT transducer. This ratio is a property of the PZT material and will not be affected by the level of impact. Therefore, the two curves in figure 8 share the same slope. However, from the experimental results, the 242 g ball provided a higher energy output than the 28 g ball when dropped with the same impact energy. This discrepancy is because for the same impact energy, the impact force of the 242 g ball is much larger than that of the 28 g ball if the impact duration is assumed the same. The larger impact force induced a larger PZT sensor output voltage, which means higher sensor output energy. This explains why the curve associated with the 242 g ball is higher than that of the 28 g ball in figure 8. It is clear from both figures 7 and 8 that the PZT sensor outputs proportionally correlate to the impact level.

#### 4.4. Health monitoring of the concrete girder

During the impact tests, health monitoring tests are conducted concurrently. Wavelet packet analysis was used as a signal-processing tool to analyse the sensor signal of the embedded PZT patch in a concrete specimen. A wavelet is a waveform of effectively limited duration that has an average value of zero:

$$\int_{-\infty}^{+\infty} \Psi(t) dt = 0. \quad (6)$$

Using a selected mother wavelet function  $\Psi(t)$ , the continuous wavelet transform (CWT) of a function  $f(t)$  is

defined as

$$W_f(a, b) = \frac{1}{\sqrt{a}} \int_{-\infty}^{+\infty} f(t) \bar{\Psi}\left(\frac{t-b}{a}\right) dt, \quad (7)$$

where  $a > 0$  and  $b \in R$  are the dilation and translation parameters, respectively. The bar over  $\Psi(t)$  indicates its complex conjugate. In wavelet analysis, a signal is split into an approximation and a detail. The approximation is then itself split into a second-level approximation and detail, and the process is repeated. In wavelet packet analysis, the details as well as the approximations can be split. The advantage of wavelet packet analysis is that it enables the inspection of relatively narrow frequency bands over a relatively short time window. In this paper, Daubechies wavelet base (db9) is used as the mother wavelet. The frequency band is not overlapped because of the orthogonality of the Daubechies wavelet base. In the proposed method, the sensor signal  $S$  is decomposed by an  $n$ -level wavelet packet decomposition into  $2^n$  signal sets,  $\{X_1, X_2, \dots, X_{2^n}\}$ , with

$$X_j = [x_{j,1}, x_{j,2}, \dots, x_{j,m}], \quad (8)$$

where  $m$  is the number of the sampling data,  $E_{i,j}$  is the energy of the decomposed signal, where  $i$  is the time index (window index), and  $j$  is the frequency band ( $j = 1, \dots, 2^n$ ).  $E_{i,j}$  is given by the equation

$$E_{i,j} = \|X_j\|_2^2 = x_{j,1}^2 + x_{j,2}^2 + \dots + x_{j,m}^2. \quad (9)$$

The energy vector at time index  $i$  is

$$E_i = [E_{i,1}, E_{i,2}, \dots, E_{i,2^n}]. \quad (10)$$

Various kinds of damage indices have been developed for health monitoring of civil structures in recent years. Root-mean-square deviation (RMSD) is a suitable damage index to compare the difference between the signatures of the healthy state and the damaged state. Soh *et al* (2000) successfully conducted RMSD between signatures of PZT transducers to form the damage index for the health monitoring of a reinforced concrete (RC) bridge. Tseng and Naidu (2002) presented the damage index by calculating the RMSD between the impedance of the PZT transducer mounted on aluminium specimens. In this paper, RMSD of the energy vector is calculated as the damage index for health monitoring purposes.

The energy vector for healthy data is denoted as  $E_h = [E_{h,1}, E_{h,2}, \dots, E_{h,2^n}]$ . The energy vector for the damage state at time index  $i$  is represented by  $E_i = [E_{i,1}, E_{i,2}, \dots, E_{i,2^n}]$ . The damage index at time  $i$  is defined as

$$I = \sqrt{\frac{\sum_{j=1}^{2^n} (E_{i,j} - E_{h,j})^2}{\sum_{j=1}^{2^n} E_{h,j}^2}}. \quad (11)$$

During the test, a sweep sinusoidal signal was used as an excitation source for the piezoceramic actuator (PZT1). The magnitude for the sweep sinusoidal signal was 20 V. The sweep sinusoidal signal starts from 100 Hz and ends at 10 kHz through a sweep period of 10 s. PZT1 was used as actuator while PZT2 and PZT3 were used as sensors.

The proposed damage index represents the transmission energy loss portion caused by damage. When the damage index

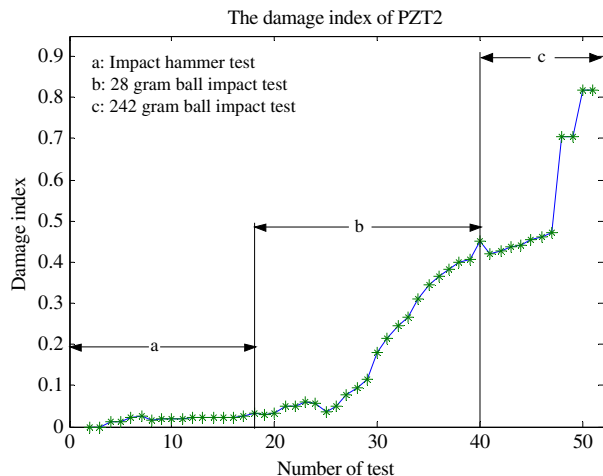


**Figure 9.** Damage index during impact hammer tests and free dropping tests for PZT2.

is close to 0, it means it is in a healthy state. The greater the index, the more severe the damage is.

During the test, the impact hammer test was performed first. After the impact hammer test, the 28 g ball impact test and 242 g ball impact test were performed until the concrete was in a severe state of damage. From the damage index history (figure 9), it can be seen that, during the impact tests, the damage index was increasing, indicating that there was increasing damage inside the sample with the repeated impact. When the damage index reached 0.45, minor cracks started to appear on the surface of the concrete specimen. At a damage index of 0.7, wider cracks were observed. At a damage index of 0.81, a severe crack was clearly present at the centre of the specimen. The width of the crack in the centre of the concrete specimen was measured to be 0.002" at the top of the specimen, 0.005" in the mid-section of the specimen and 0.015" at the bottom of the specimen. Figure 9 clearly demonstrated that the damage index can be used to represent the damage status of the concrete specimen.

## 5. Conclusion

An overheight truck–bridge collision detection and evaluation system is developed using piezoceramic transducers. Piezoceramic transducers were used for impact detection and health monitoring purposes. An electric circuit is designed to detect the impact and activate a digital camera to take photos of an offending truck as it collides with the concrete bridge. The output of the impact sensing PZT sensor is proportional to the impact energy when collision is simulated in impact tests. Impact levels can be estimated from the impact sensor signal. The PZT-based health monitoring method can also detect the growth of cracks inside the concrete structure when the structure is gradually damaged in repeated impact tests. The proposed overheight truck–bridge collision detection and evaluation system

has the functions of simultaneously sending a triggering signal to capture an image of the offending vehicle, estimating the impact level and evaluating the damage level of the bridge. The proposed system has the potential to be applied to highway overpass bridges as an integrated structural system to provide extended safety monitoring and accident notification.

## Acknowledgments

This research is partially supported by a grant (State Job no. 134142) from the Ohio Department of Transportation via the University of Akron. Special thanks go to Dr P Qiao, who is the PI of this project.

## References

- Ayres J W, Lalande F, Chaudhry Z and Rogers C 1998 Qualitative impedance-based health monitoring of civil infrastructures *Smart Mater. Struct.* **7** 599–605
- Egusa S and Iwasawa N 1998 Piezoelectric paints as one approach to smart structural materials with health-monitoring capabilities *Smart Mater. Struct.* **7** 438–45
- Galea C S, Chiu W K and Paul J J 1993 Use of piezoelectric films in detecting and monitoring damage in composites *J. Intell. Mater. Syst. Struct.* **4** 683–9
- Lee C K, Lin C T, Hsiao C C and Liaw W C 1998 New tools for structural testing: piezoelectric impact hammers and acceleration rate sensors *J. Guid. Control Dyn.* **21** 692–7
- Lorenz R D, Bannister M, Daniel P M, Krysiniski Z, Leese M R, Miller R J, Newton G, Rabbetts P, Willett D M and Zarnecki 1994 An impact penetrometer for a landing spacecraft *Meas. Sci. Technol.* **5** 1033–41
- Quek S T, Wang Q, Zhang L and Ong K H 2001 Practical issues in the detection of damage in beams using wavelets *Smart Mater. Struct.* **10** 1009–17
- Saafi M and Sayyah T 2001 Health monitoring of concrete structures strengthened with advanced composite materials using piezoelectric transducers *Composites B* **32** 333–42
- Sendra A S and Smith C K 1998 *Microelectronic Circuits* 4th edn (New York: Oxford University Press)
- Soh C H, Tseng K K, Bhalla S and Gupta A 2000 Performance of smart piezoceramic patches in health monitoring of a RC bridge *Smart Mater. Struct.* **9** 533–42
- Song G, Gu H, Mo Y L, Hsu T T C, Dhonde H and Zhu R H 2004 Health monitoring of a reinforced concrete bridge bent-cap using piezoceramic materials *Proc. 3rd European Conf. on Structural Control (Vienna, July 2004)*
- Song G, Gu H, Mo Y L, Hsu T T C, Dhonde H and Zhu R H 2005 Health monitoring of a concrete structure using piezoceramic material *SPIE Int. Symp.—Smart Structures & Materials/NDE (San Diego, CA)*
- Tong J H, Wu T T and Lee C K 2002 Fabrication of a piezoelectric impact hammer and its application to the *in situ* nondestructive evaluation of concrete *Japan. J. Appl. Phys.* **41** 6595–600
- Tseng K K-H and Naidu A S K 2002 Non-parametric damage detection and characterization using smart piezoceramic material *Smart Mater. Struct.* **11** 317–29
- Tseng K T and Wang L 2004 Smart piezoelectric transducers for *in situ* health monitoring of concrete *Smart Mater. Struct.* **13** 1017–24
- Wang S C, Wu F and Chang F-k 2001 Structural health monitoring from fiber-reinforced composites to steel-reinforced concrete *Smart Mater. Struct.* **10** 548–52